Published by SET Publisher

Journal of Basic & Applied Sciences

ISSN (online): 1927-5129

Sensitivity Analysis of Wind Turbine Broadband Noise Estimation to Semi-Empirical Models Parameters

Filippo De Girolamo*, Lorenzo Tieghi, Giovanni Delibra, Alessio Castorrini and Alessandro Corsini

Department of Mechanical and Aerospace Engineering, Sapienza University, Via Eudossiana 18, 00154, Rome, Italy

Article Info:

Keywords:
Wind turbine rotor noise,
semi-empirical noise models,
Trailing edge noise,
Inflow noise.

Citation: De Girolamo F, Tieghi L, Delibra G, Castorrini A, Corsini A. Sensitivity analysis of wind turbine broadband noise estimation to semi-empirical models parameters. J Basic Appl Sci 2023; 19.

Abstract:

The continuous increase of energy demand and the rising concerns on climate change, are pushing the European Union decarbonization strategies and transition toward renewable based energy systems, with wind energy playing a leading role. It is therefore necessary to have a better understanding of how wind turbines (WTs) impact on their surroundings, including their noise emissions. Among the different methods to compute noise emissions of WTs, semi-empirical models are a valid choice to have a-priori estimations of noise spectra and sound pressure levels. These models are based on correlation laws for different physical mechanisms that contribute to noise generation. Popular models for dominant noise sources include the Amiet approach for inflow turbulence noise and the Lowson model for turbulent boundary layer-trailing edge noise. Determining the parameters involved in these models can be challenging, potentially leading to significant errors in noise prediction. In this study, we conducted a novel sensitivity analysis of the models by varying different parameters such as turbulent intensity and dissipation, boundary layer thickness, and temperature. The selected test case is the reference multi-MW horizontal axis wind turbine Neg-Micon 80. The results of the multilevel-multivariate analysis, involving 63,360 combinations of the input parameters, clearly demonstrate a significant dependence of these models on atmospheric turbulence parameters. Furthermore, these models exhibit an higher sensitivity to input parameters at lower frequencies of the noise spectrum, which are generally associated with higher values of sound pressure level.

*Corresponding Author
E-mail: filippo.degirolamo@uniroma1.it

1. INTRODUCTION

The increasing penetration of wind turbines and farms in human populated areas raises concerns regarding their impacts on environment and population. In particular, the noise emissions generated by rotors may negatively interfere with local human activities [1]. Even if some authors agree that most of the rotor aerodynamic noise is masked by environmental background noise [2], the researches from Bakker *et al*. have found psychological distress and sleep disturbances in populations leaving in close proximity of wind turbines [3]. In addition, noise emissions from wind farms and turbines must comply with regional and national regulations [4].

Acoustic emissions from wind turbines can be classified into mechanical and aerodynamic noises. While manufacturers can easily control the former through precautionary measures, the latter is dependent on the inevitable interaction between the wind and the turbine itself. Furthermore, it is worth noting that aerodynamic noise increases with rotor size. Although the understanding of rotor aerodynamic noise mechanisms is not yet fully comprehensive, a majority of authors agree in acknowledging that noise predominantly originates from interaction between leading edge and the atmospheric turbulence (*inflow turbulence noise*) and the wake generated at the trailing edge (*airfoil self-noise*) [5].

However, noise prediction of wind turbines can result in complex and computationally expen- sive numerical campaigns. Few experimental data are available, and numerical simulations based on medium- and high-fidelity approaches require demanding HPC efforts [6]. On the contrary, semi-empirical acoustic models (SAMs) are able to estimate the acoustic spectrum and sound pressure level (SPL) by setting a few parameters and operating conditions of the turbine [7]. A review of the main models can be found in Bhargava *et al*. [8]. For instance, Leloudas *et al*. [9] combined Blade-Element Momentum (BEM) method and semi-empirical models with mea- surements to estimate noise emissions from a wind turbine test site, obtaining a good agreement between measured and computed noise spectrum. A similar approach can be found in Zhu *et al*. [10], where they compared the Brooks-Pope-Marcolini model [11] for airfoil self-noise prediction with measurements from a small-sized wind turbine. The results clearly show that accurate eval- uation of the boundary layer thickness enhances the accuracy of noise prediction. De Girolamo *et al*. [12] combined the actuator line method through URANS approach with SAMs to have an accurate estimation of WT self-noise.

Despite the widespread use of SAMs in the literature, the predicted sound pressure level (SPL) can be significantly influenced by some of the assumptions made by the user. For in- stance, the Amiet model [13] for turbulence inflow noise relies on selecting appropriate values for the turbulent length scale and turbulent intensity. These parameters often need to be sta- tistically derived from extensive measurement campaigns conducted over a long period of time. When it comes to airfoil self-noise, Lowson's model [8] for turbulent boundary layer-trailing edge interaction, also poses certain challenges. Specifically, it requires the modeling of the boundary layer thickness, which is difficult to estimate in advance.

The aim of this work is to conduct a novel sensitivity analysis of the broadband noise estimation given by Amiet and Lowson semi-empirical models, to typical model input parameters. Turbulent intensity and dissipation, boundary layer thickness, and temperature, were linearly varied to compute SPL for each input combination. Uni-, bi- and multi-variate comparison are then carried out to gain insights into parameters' impact on the overall SPL prediction.

2. SEMI-EMPIRICAL MODELLING OF ROTOR NOISE

Noise emissions in wind turbines as well as in ducted turbomachinery can be ascribed to mechanical and aerodynamic noise, with the latter being predominant. Among the various mechanisms that concur to the noise level, the two dominant sources come from the interaction (i) between WT blades and turbulent inflow, *i.e. inflow-turbulence noise*, and (ii) between the sharp edges of the trailing edges and the turbulent vorticity in the boundary layer, *i.e. turbulent bound- ary layer-trailing edge noise* [10]. The two mechanisms can be estimated using semi-empirical models. The overall SPL can therefore be computed as:

$$SPL_{overall} = 10\log_{10}\left(10^{0.1\cdot SPL_{TI}} + 10^{0.1\cdot SPL_{TE}}\right) \quad (1)$$

where SPL_{TI} and SPL_{TE} are the contribution for inflow turbulence and turbulent boundary layer-trailing edge noises respectively. The formulation for inflow-turbulence noise follows the approach of Amiet [14], that expresses the SPL as one-third octave bands at a given frequency as:

$$SPL_{TI} = 10\log_{10}\left(\rho^2 c^4 \frac{L_{\in} d}{2r_e^2} M^5 T_I^2 \frac{\hat{k}^3}{(1+\hat{k}^2)^{\frac{7}{3}}} \bar{D}\right) + 78.4 \quad (2)$$

where ρ is the air density, c is the wind velocity, L_ϵ is the turbulent dissipation length scale, d is the blade span, r_e is the distance between receiver and source, M the local Mach number, T_I the turbulent intensity. $\bar{D}$ is a directivity term that keeps in account the position of the receiver, whereas the wavelength $\hat{k}$ can be computed as:

$$k = \frac{4}{3} \bullet \frac{2\pi f K_{\in}}{U} \quad (3)$$

The model has been additionally modified to improve its accuracy at lower frequencies, according to [15].

Based on the Lowson model [8], the SPL due to trailing-edge noise can be estimated as:

$$SPL_{TE} = 10\log_{10}\left(\frac{\delta M^5 d}{r_e^2} G(f)\right) + 128.5 \quad (4)$$

where the function $G(f)$ reads as:

$$G(f) = \frac{4\left(\frac{f}{f_p}\right)^{2.5}}{\left[\left(\frac{f}{f_p}\right)^{2.5} + 1\right]^2} \quad (5)$$

The Strouhal peak frequency f_p is a function of the Mach number and boundary layer displacement thickness δ^*, such as:

$$f_p = \frac{0.02U\ M^{-0.6}}{\delta^*} \quad (6)$$

In the original formulation, the boundary layer displacement thicknesses is estimated based on the boundary layer thickness δ, derived from the flat plate theory:

$$\delta^* = 0.125\delta = 0.125(0.37\,\mathrm{Re}^{-0.2}) \quad (7)$$

3. METHODOLOGY

The two semi-empirical models have been implemented within an in-house made Python-v3.8 framework, shown in Figure **1**. The inputs to the framework can be divided into environmental, depending on the wind conditions, e.g. wind speed, ambient temperature and pressure, and geometric parameters. In fact, following this approach the blades of the WTs are discretized in a series of blade elements determined by properties as chord length, thickness, boundary layer thickness. The two noise models, i.e. Lowson and Amiet, are fed with the input data and computed for a single blade element, with their outputs summed using a logarithmic operator, to compute the $SPL_{overall}$ for the blade element. The process is iterated over the blade elements, obtaining the overall SPL of the turbine. Results are eventually stored in a hierarchical dataset. The 2.75 MW Neg-Micon NM80 horizontal-axis wind turbine (WT), as referenced in [16] and [17], was used for the study. The 40.04 m long blade is discretized in 28 elements. Boundary layer thickness δ, turbulent intensity T_I, dissipation length L_ϵ, and temperature T were varied as indicated in Table **1**, for a total of 63,360 trials. Calculations required 36 hours on an AMD Opteron 6380.

The parameter limits were determined based on previous investigations reported in [12]. Specifically, the angle of attack and Reynolds number were obtained through Reynolds-Averaged Navier-Stokes simulations. The Actuator Line Method was used to reproduce the wind turbine rotor, considering the rated operational conditions outlined in [18]. Consequently, the limits for the boundary layer thickness were derived using XFoil [19], taking into account the variability range of the angle of attack and Reynolds number. Turbulent intensity and temperature were selected within a range of typical environmental conditions typical of wind turbine operations. The temperature directly impacts the calculation of density ρ and speed of sound c, which are computed assuming standard atmospheric pressure (101325 *Pa*). The minimum considered value of the dissipation length is 10 m, as the semi-empirical acoustic models require the assumption of a compact acoustic source, which is valid when the atmospheric dissipation length significantly exceeds the characteristic chord dimensions of the blade (with a maximum value of approximately 3 m in this case).

4. UNIVARIATE ANALYSIS

Casalino *et al*. presented in [20] an exhaustive comparison of different codes by the participants of IEA Wind Task 29 and 39 [18, 21]. These tasks specifically focused on the benchmark configuration of the NM80 wind turbine. Among these codes, we chose to compare our results with numerical data obtained from

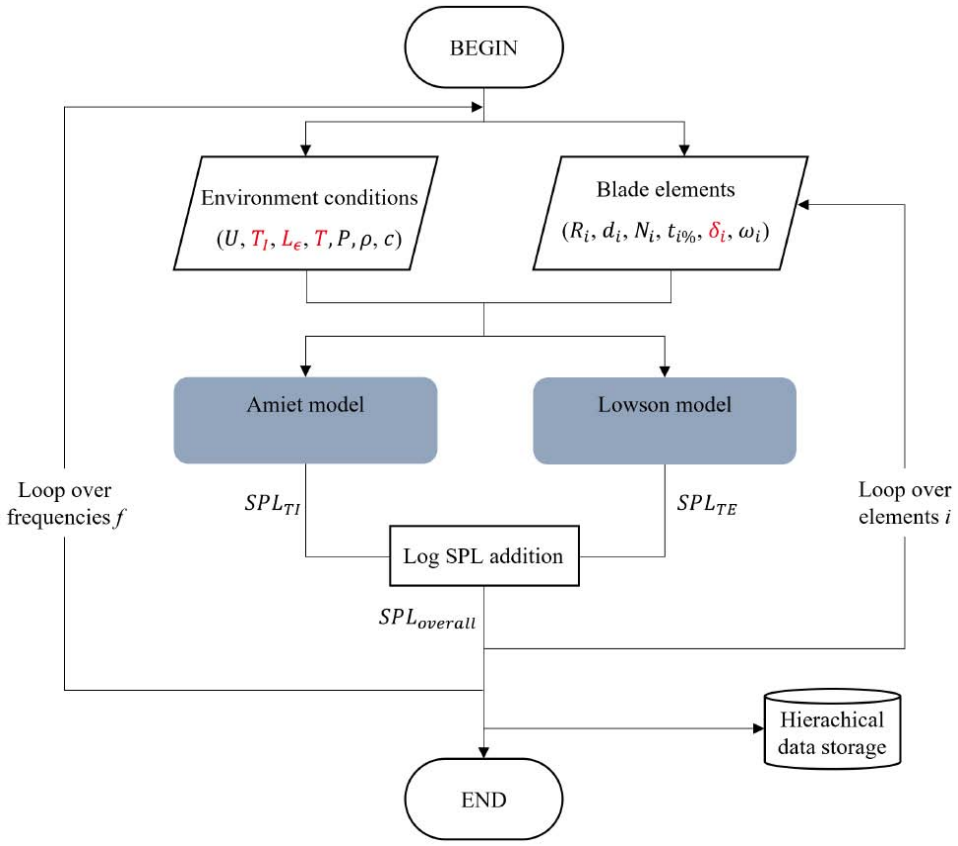

Figure 1: Scheme of the Python framework for overall SPL computation.

the NAFNoise code developed by Moriarty *et al*. [22] from the National Renewable Energy Laboratory (NREL).

Table 1: Variability Range of the Factors Included in the Analysis

Variable	Min value	Max value	Step
δ [m]	0.01	0.08	0.005
T_I [%]	1	30	1
T [$^\circ C$]	-10	40	5
L_c [m]	10	120	10

A first characterization of the influence of the models' factors on the computed SPL can be performed by analyzing the SPL spectra reported in Figure **2**. These spectra are obtained by varying the values of a factor and setting the remaining variables to a fixed value. The variation of the temperature shows a mild influence on the predicted SPL, that increases from 42 dB to 44 dB for the peak value by reducing atmospheric temperature from 40 ˚C to 10 ˚C. This leads to the conclusion that an incorrect selection of the other variables may lead to a strong underprediction of the noise emissions of the rotor. The semi-empirical aeroacoustics formulations shows instead a strong dependency on the boundary layer thickness δ. In particular, as this thickness is increased, the peak frequency moves at lower frequencies, suggesting that large errors in the estimations of δ reflects in incorrect prediction of the spectrum shape. Lower values of δ are also associated to a lower SPL; for instance SPL varies from 40.2 dB in the case of δ = 1 cm to 44.2 dB computed with δ = 8 cm. Both the dissipation length L_ϵ and the turbulent intensity T_I strongly affect the SPL prediction, as evident from Figure **2c** and **d**. Particularly, by increasing the estimation of T_I from the lower bound (1%) to the chosen maximum (10%) a significant increase in SPL is achieved, from 40 dB to 47 dB. The increase in dissipation length instead reflects in a reduction in SPL. However, the comparison with reference data highlights that careful selection of the T_I is necessary to achieve a reliable result in terms of noise spectrum.

5. BI- AND MULTI-VARIATE ANALYSIS

A multi-dimensional map for the overall SPL was built based on the results from parametric analysis. It allows an estimation of the relative weights between

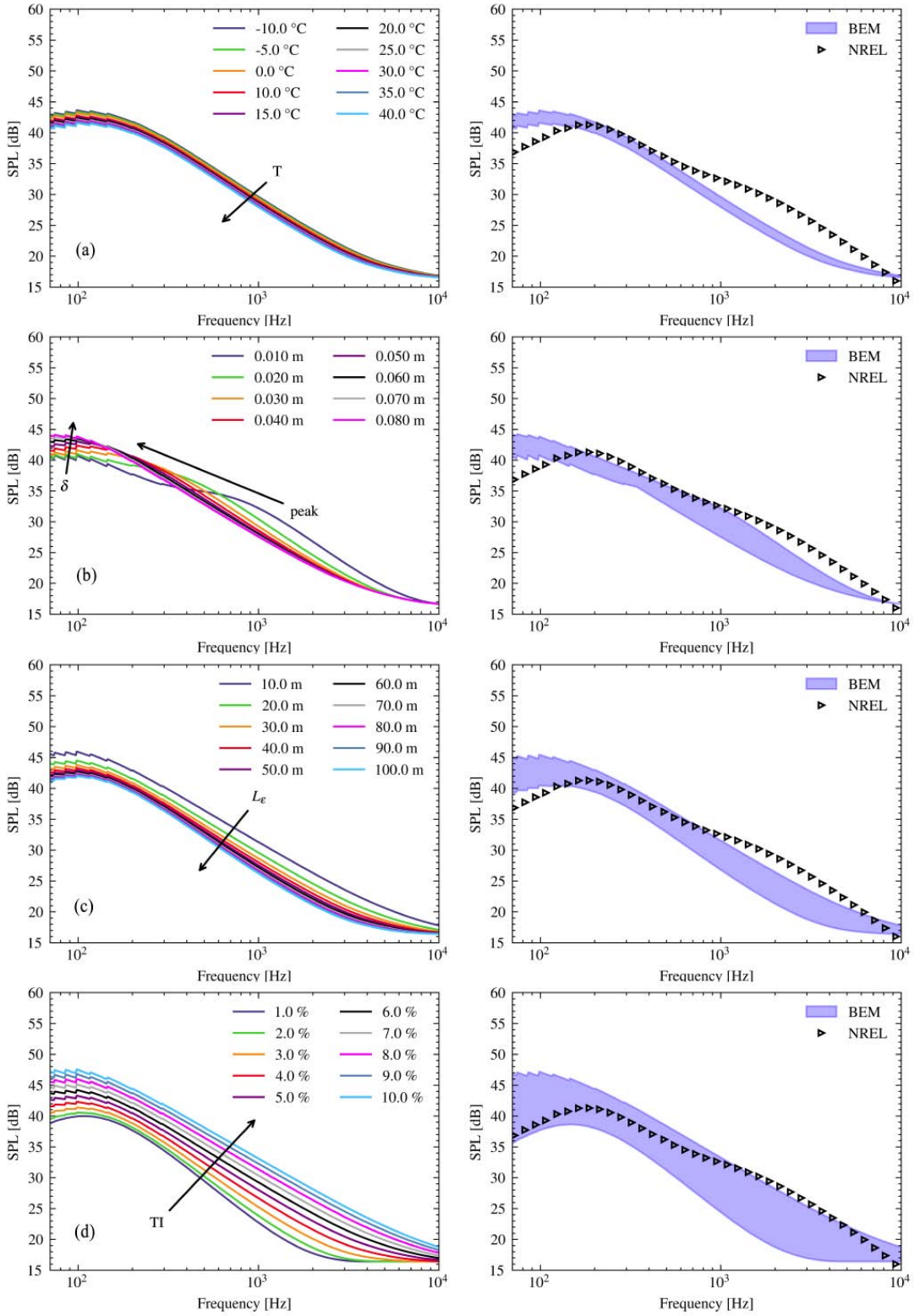

Figure 2: Predicted SPL spectra as a function of a single variable for fixed combination of the other parameters: (**a**) T_I = 5%, L_ϵ = 40 m, δ = 0.04 m (**b**) T_I = 5%, L_ϵ = 40 m, T = 20 ˚C (**c**) T_I = 5%, δ = 0.05 m, T = 20 ˚C (**d**) L_ϵ = 40 m, δ = 0.05 m, T = 20 ˚C and comparison with numerical data from [20] (T_I = 5%, L_ϵ = 39 m, T = 14 ˚C).

parameters. Some of the significant combinations and their effects on the overall SPL is reported in Figure **3**. The different subplots illustrate the SPL as a function of two variables, with fixed combinations of the remaining factors. The analysis of results suggests that some factors have a drastic impact on the predicted SPL,

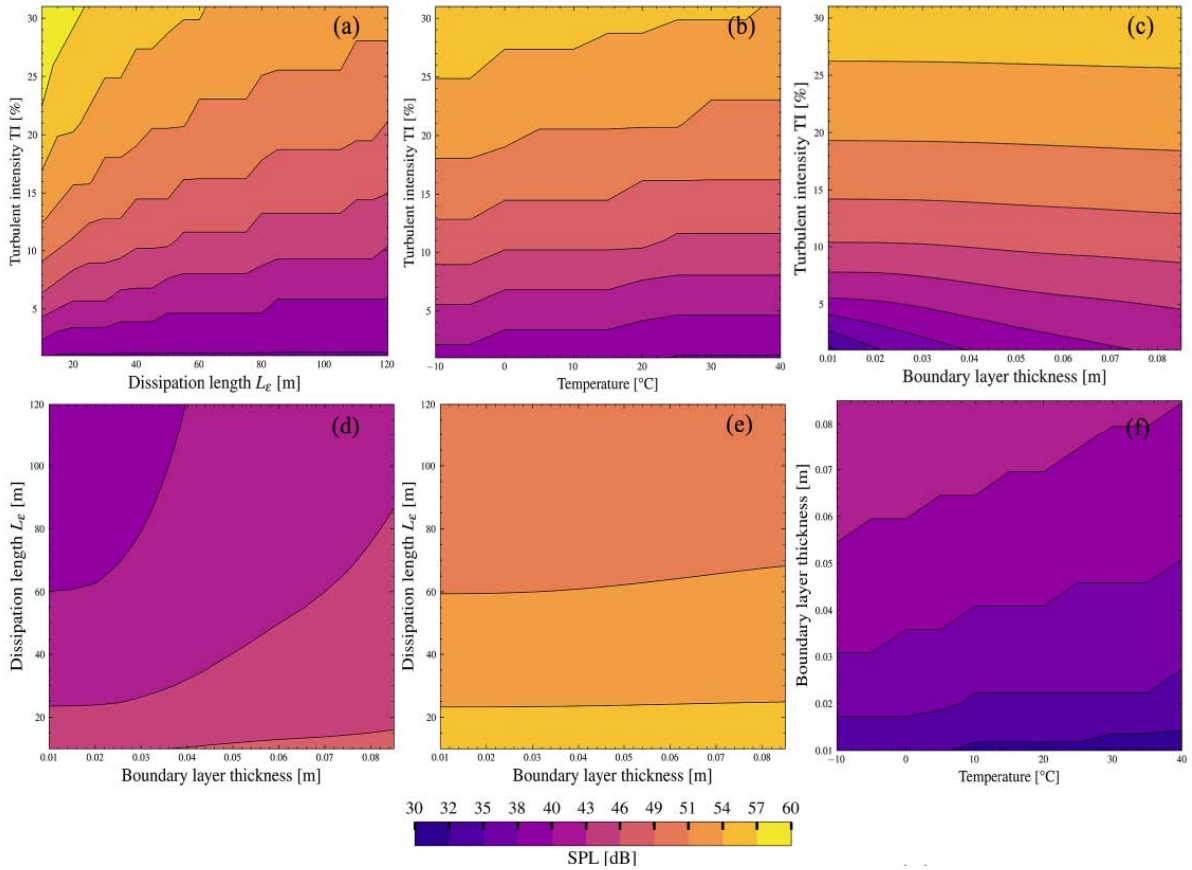

Figure 3: Overall SPL variability for fixed combination of parameters: (**a**) $L_\epsilon - T_I$, δ = 0.02 *m*, T = 20 ˚C (**b**) $T - T_I$, δ = 0.02 *m*, L_ϵ = 40 *m* (**c**) $\delta - T_I$, T = 20 ˚C, L_ϵ = 40 *m* (**d**) $\delta - L_\epsilon$, T = 20 ˚C, T_I = 6% (**e**) $\delta - L_\epsilon$, T = 20 ˚C, T_I = 6% (**f**) $T - \delta$, T_I = 1%, L_ϵ = 40 *m*.

while large variation of others do not affect the outcome significantly. In particular:

- Dissipation rate and turbulent intensity play a significant role, as small variations lead to large variations of the SPL peak. This can be observed in Figure **3a**, where SPL drops from 60 dB to 30 dB. This may seriously impair SAM applicability to a case where no accurate data on inflow turbulence are available.

- As a consequence of the Amiet formulation, the SPL increases drastically for high values of turbulent intensity, and it is dominant in the overall SPL prediction with respect to temperature, Figure **3b**, and δ for T_I > 5%, Figure **3c**.

- Temperature has a mild influence on the SPL, as evident from 3 (b) and (f), with a noticeable effect only at extreme values (-10/40 ˚C).

- The boundary layer thickness δ shows a certain degree of correlation with the dissipation length selection Figure **3d**, resulting in an intermediate variation of the SPL from 38 dB (low δ and L_ϵ > 90*m*) to 45-50 dB (L_ϵ < 5*m*). Nevertheless, such correlation can be totally neglected for high values of turbulent intensity (T_I > 20%).

The contribution of inflow noise (Amiet model) and turbulent boundary layer-trailing edge noise (Lowson model) to the SPL for whole space of simulations is reported in Figure **4** at four characteristic frequencies. The results highlight that, regardless of the wave frequency that is considered, the Amiet contribution toward overall SPL is dominant for high levels of noise. The statistical description of the SPL is reported in Table **2**, and shows that the average SPL shows a tendency to decrease with frequency, whereas the standard deviation is also reduced accordingly. This observation also suggests that errors resulting from uncertainties in the input model parameters have a greater impact at lower frequencies, which are associated with higher values of SPL.

At frequencies above 1000 Hz the Lowson model has a milder dependency from the variation of model inputs, with the range of computed $SPL_{T\,E}$ that ranges from 11

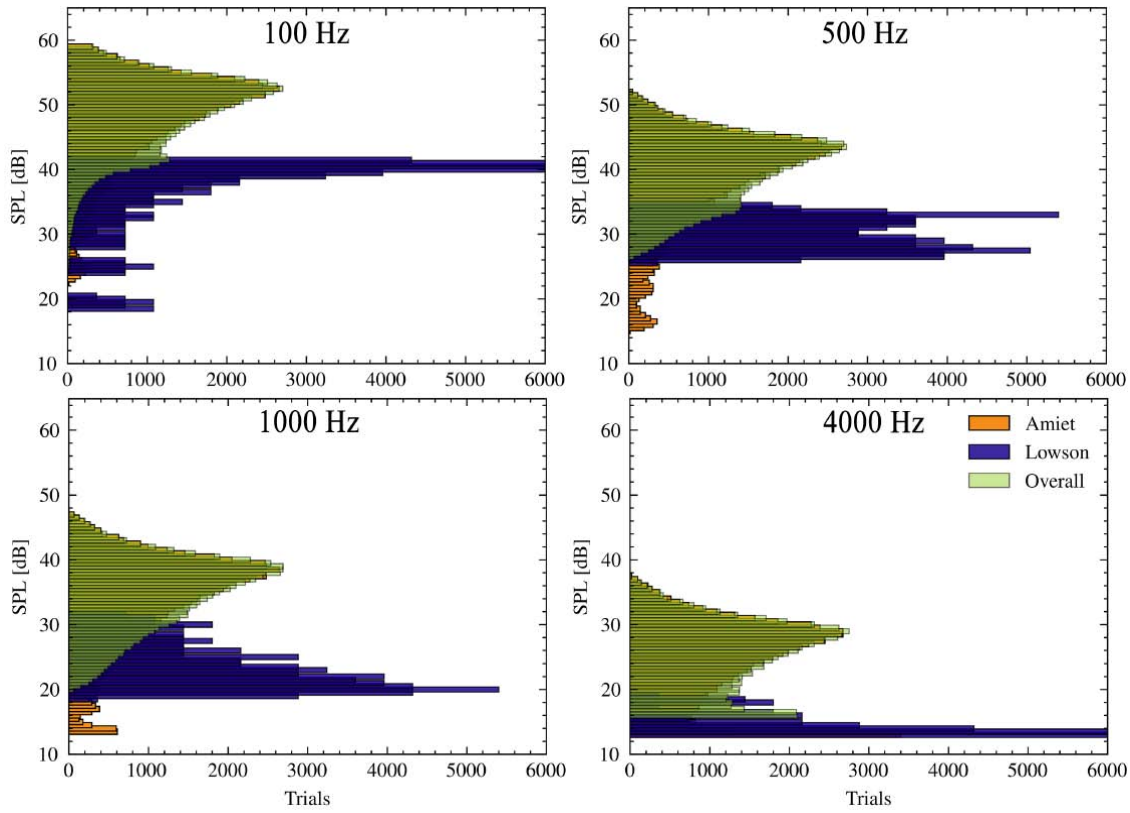

Figure 4: SPL distribution over the total combination of imput parameters (63,360 trials) of overall inflow turbulence (Amiet), turbulent boundary layer-trailing edge noise (Lowson) and overall computed SPL at characteristic noise frequencies of 100, 500, 1000 and 4000 Hz.

Table 2: Values of Means and Standard Deviations Over the Total Trials of Semi-Empirical Models and Overall Noise Spectra

Frequency [Hz]	Amiet		Lowson		Overall	
	Mean [dB]	SD [dB]	Mean [dB]	SD [dB]	Mean [dB]	SD [dB]
100	47.74	7.58	36.13	6.28	48.99	5.78
500	38.62	7.47	30.28	2.49	40.22	5.23
1000	33.88	7.25	23.78	3.47	35.15	5.56
4000	24.74	5.96	14.18	1.39	25.52	5.09

dB to 18.7 dB at 4000 Hz, with respect of the broader distribution that is instead observed at 100 Hz, At the lowest frequency (100 Hz), the distribution has two peaks at 43 dB and 57 dB, with a wide range of calculated values spanning from 35 to 60 dB.

These two peaks arise from the separated effects of the semi-empirical models on the overall acoustic spectrum. Specifically, the noise generated by turbulent inflow carries more weight than the turbulent boundary layer-trailing edge noise in the overall noise spectrum due to its higher SPL values. Variability of turbulent-inflow noise (Amiet formulation) shows generally a large variability to the input variations, exhibiting a higher standard deviation than the Lowson model (Table **2**). However, similarly to the latter, the uncertainty of the model is reduced as frequency increases.

6. CONCLUSIONS

The sensitivity analysis of SPL prediction for HAWTs through semi-empirical acoustics models was conducted to assess the impact of four key parameters: turbulent dissipation length (L_ϵ), turbulent intensity (T_I), boundary layer thickness (δ), and temperature (T). These models are an effective alternative to more accurate but computationally expensive CAA methods.

An in-house Python framework was employed to assess the main aerodynamic noise mechanisms. The evaluation included the Amiet model for turbulent inflow noise and the Lowson model for turbulent boundary layer-trailing edge noise. A comprehensive range of values was considered for each of the aforementioned parameters, resulting in a total of 63,360 trials. The study focused on the reference Neg-Micon NM80 wind turbine.

The univariate analysis revealed that turbulent intensity and dissipation length are the parameters that have the greatest influence on SPL prediction. On the other hand, the uncertainties caused by temperature and boundary layer thickness misprediciton are lower in terms of maximum SPL level, although increasing boundary layer thickness induces a shift of the overall SPL peak to lower frequencies, severely changing the shape of the spectrum. In addition, the calculations were compared with results from NREL, as reported in [20], using the NM80 benchmark configuration prescribed in the IEA Wind Task 29 and 39.

Contour plots from the bivariate analysis underlined the impact of the turbulent intensity and dissipation length, showing that small changes in these parameters can lead to a drop up to 30 dB. This underscores the importance of precise measurements of atmospheric parameters in obtaining accurate predictions of SPL using SAMs. There appears to be a slight correlation between boundary layer thickness and dissipation length, but this correlation becomes negligible for turbulent intensities higher than 20%. Furthermore, the increase in dissipation length results in a decrease of the maximum value of the overall SPL across the whole frequency spectrum.

The Amiet contribution to the overall SPL is dominant regardless of the frequency. That can be confirmed observing the entire simulation space at characteristic noise frequencies of 100, 500, 1000, and 4000 Hz, which exhibit that the Amiet model generally generates higher values of SPL than the Lowson model. The standard deviation decreases as the frequency increases, indicating that the semi-empirical acoustic models are more sensitive to input parameters at lower frequencies.

ACKNOWLEDGEMENTS

This research is supported by the Ministry of University and Research (MUR) as part of the PNRR, Spoke 6 “Multiscale Modelling and Engineering Application” in CN1-HPC “National Center on HPC, Big Data and Quantum Computing”.

NOMENCLATURE

$\bar{D}$	Directivity	[−]
δ	Boundary layer thickness	[m]
δ^*	Boundary layer displacement thick	[m]
ρ	Density	[kg/m^3]
c	Speed of sound	[m/s]
d	Span	[m]
f	Frequency	[Hz]
f_p	Peak frequency	[Hz]
k	Wavenumber	[$1/m$]
L_ϵ	Dissipation length	[m]
M	Mach number	[−]
N	Number of ALM elements	[−]
P	Pressure	[Pa]
R	Radius	[m]
r_e	Source-receiver distance	[m]
T	Temperature	[$^\circ$C]
$t_{\%}$	Airfoil thickness	[−]
T_I	Turbulence intensity	[−]
U	Mean velocity	[m/s]

REFERENCES

[1] Qu F, Tsuchiya A. Perceptions of wind turbine noise and self-reported health in suburban residential areas. Frontiers in Psychology 2021; 12: 736231. https://doi.org/10.3389/fpsyg.2021.736231

[2] Katinas V, Marčiukaitis M, Tamašauskiene M. Analysis of the wind turbine noise emissions and impact on the environment. Renewable and Sustain- able Energy Reviews 2016; 58: 825-831. https://doi.org/10.1016/j.rser.2015.12.140

[3] Bakker RH, *et al.* Impact of wind turbine sound on annoyance, self-reported sleep disturbance and psychological distress. Science of the Total Environment 2012; 425: 42-51. https://doi.org/10.1016/j.scitotenv.2012.03.005

[4] Peeters IB, Nusselder R. Overview of critical noise values in

the European Region. In: EPA Network Interest Group on Noise Abatement (IGNA): Vught, The Netherland 2019; p. 182.

[5] Wagner S, Bareiss R, Guidati G. Wind turbine noise. Springer Science & Business Media 2012.

[6] Lele SK, Nichols JW. A second golden age of aeroacoustics? Philosophical Transactions of the Royal Society A: Mathematical, Physical and Engineering Sciences 2014; 372(2022): 20130321. https://doi.org/10.1098/rsta.2013.0321

[7] Zhu WJ, *et al.* Wind turbine noise generation and propagation modeling at DTU Wind Energy: A review. Renewable and Sustainable Energy Reviews 2018; 88: 133-150. https://doi.org/10.1016/j.rser.2018.02.029

[8] Nukala VB, Padhy CP. Concise review: aerodynamic noise prediction methods and mechanisms for wind turbines. International Journal of Sustainable Energy 2023; 42(1): 128-151. https://doi.org/10.1080/14786451.2023.2168000

[9] Leloudas G, *et al.* Prediction and reduction of noise from a 2.3 MW wind turbine. In: Journal of physics: conference series. IOP Publishing 2007; Vol. 75(1): p. 012083. https://doi.org/10.1088/1742-6596/75/1/012083

[10] Zhu WJ, *et al.* Modeling of aerodynamically generated noise from wind turbines 2005. https://doi.org/10.1115/1.2035700

[11] Brooks TF, Pope DS, Marcolini MA. Airfoil self-noise and prediction. Tech Rep 1989.

[12] De Girolamo F, *et al.* Surrogate modeling of aeroacoustics of NM80 wind turbine 2023.

[13] Amiet RK. Acoustic radiation from an airfoil in a turbulent stream. Journal of Sound and Vibration 1975; 41(4): 407-420. https://doi.org/10.1016/S0022-460X(75)80105-2

[14] Bortolotti P, *et al.* Aeroacoustics noise model of OpenFAST. Tech. Rep. National Renewable Energy Lab. (NREL), Golden, CO (United States) 2020.

[15] Moriarty P, Migliore P. Semi-empirical aeroacoustic noise prediction code for wind turbines. Tech. rep. National Renewable Energy Lab., Golden, CO. (US) 2003. https://doi.org/10.2172/15006098

[16] Madsen HA, *et al.* The DAN-AERO MW experiments. Final report 2010. https://doi.org/10.2514/6.2010-645

[17] Schepers JG, *et al.* IEA Wind TCP Task 29, Phase IV: Detailed Aerodynamics of Wind Turbines 2021.

[18] Bertagnolio F, *et al.* IEA Wind TCP-Task 29 T3. 7 & Task 39 Wind Turbine Noise Code Benchmark-Preliminary Results 2021.

[19] Drela M. XFOIL: An analysis and design system for low Reynolds number airfoils. In: Low Reynolds Number Aerodynamics: Proceedings of the Conference Notre Dame, Indiana, USA, 5–7 June 1989. Springer 1989; pp. 1-12. https://doi.org/10.1007/978-3-642-84010-4_1

[20] Casalino D, van der Velden WC, Romani G. A Framework for Multi-Fidelity Wind-Turbine Aeroacoustic Simulations. In: 28th AIAA/CEAS Aeroacoustics 2022 Conference 2022; p. 2892. https://doi.org/10.2514/6.2022-2892

[21] Bertagnolio F. DTU Wind, and Eoin King. “TASK 39”. In: IEA Wind p. 50.

[22] Moriarty P. NAFNoise user’s guide. In: National Wind Technology Center, National Renewable Energy Laboratory 2005.